Research Square

Preprints are preliminary reports that have not undergone peer review.
They should not be considered conclusive, used to inform clinical practice,
or referenced by the media as validated information.

Insulation Failure and Partial Discharge Mechanisms of BOPP Films Under Complex Electrical Stresses

Xucheng Wang
State Grid Shandong Electric Power Research Institute
Mengzhao Zhu
State Grid Shandong Electric Power Research Institute
Qingdong Zhu
State Grid Shandong Electric Power Research Institute
Longlong Li
imlilonglong@163.com

State Grid Shandong Electric Power Research Institute

Article

Keywords: Capacitor, BOPP Films, High-Frequency Harmonic, Partial Discharge

Posted Date: August 28th, 2026

DOI: https://doi.org/10.21203/rs.3.rs-10684647/v1

License: This work is licensed under a Creative Commons Attribution 4.0 International License.
Read Full License

Additional Declarations: No competing interests reported.

Version of Record: A version of this preprint was published at Scientific Reports on November 4th, 2026.
See the published version at https://doi.org/10.1038/s41598-026-78224-8.

Insulation Failure and Partial Discharge Mechanisms of BOPP Films Under Complex Electrical Stresses

Xucheng Wang, Mengzhao Zhu, Qingdong Zhu and Longlong Li*

State Grid Shandong Electric Power Research Institute, Jinan, China; imwangxucheng@163.com (X.C.); imzhumengzhao@163.com (M.Z.); imzhuqingdong@163.com (Q.Z.)

* Correspondence: imlilonglong@163.com (L.L.)

Abstract

Parallel capacitors across the interrupter contacts of circuit breakers in ultra-high-voltage (UHV) converter stations can be exposed to power-frequency voltage with superimposed harmonics and elevated operating temperatures. To examine the associated insulation response, this study used biaxially oriented polypropylene (BOPP) films and established an electro-thermal test platform for breakdown and partial discharge (PD) measurements under power-frequency voltage, selected characteristic harmonics (550 and 650 Hz), selected high-frequency harmonics (10 and 20 kHz), harmonic proportions of 1%-5%, and temperatures of 45-85 ℃. Within this test matrix, adding harmonics was associated with lower characteristic breakdown and PD inception field strengths than the power-frequency reference in most comparisons, although the dependence on harmonic proportion was not monotonic for all characteristic-harmonic conditions. Within the high-frequency subset, the measured field strengths were generally lower at 20 kHz than at 10 kHz under matched proportions. Increasing temperature reduced the characteristic breakdown field strength across the tested harmonic conditions; the PD inception field strength was generally lower at elevated temperatures, but some temperature sequences overlapped or were non-monotonic. PRPD and PRPS patterns also varied with waveform. These conclusions provide a solid theoretical reference for insulation condition assessment and fault prevention and control of converter station parallel capacitors.

Keywords: Capacitor; BOPP Films; High-Frequency Harmonic; Partial Discharge

1 Introduction

Parallel capacitors across circuit breaker interrupter contacts in the filter bay of ultra-high voltage (UHV) converter stations are core system components, serving the key functions of optimizing electric field distribution across interrupter contacts, equalizing inter-contact

voltage distribution, and suppressing the rise rate of switching overvoltages. Their insulation reliability directly affects the stable operation of power grids [1-3].

In practical operation, in addition to withstanding long-term power-frequency operating voltage, these capacitors are continuously subjected to the superposition of 12k±1 order characteristic harmonics generated by 12-pulse commutation of converter valves and high-frequency harmonics induced by switching operations. As a result, capacitors persistently operate under complex multi-factor coupled conditions involving electric field and temperature, and their insulation systems face severe electrical stresses far exceeding design expectations [4-6].

Capacitors are categorized into three main types: electrolytic capacitors, ceramic capacitors, and organic film capacitors [7-10]. Among them, organic film capacitors can be further divided into metal foil film capacitors and metallized film capacitors (MFCs) according to electrode fabrication processes [11-12]. Benefiting from superior electrical properties including high breakdown field strength, high energy storage density, and low dielectric loss, metallized film capacitors have become the mainstream technical solution in the power capacitor sector and are widely deployed in UHV converter station filter bays [13-15].

As the core insulating medium of circuit breaker parallel capacitors, the insulation condition of BOPP films directly determines equipment operational reliability [16-21]. Partial discharge (PD) is one of the primary causes of insulation degradation in metallized film capacitors. Continuous PD accumulation progressively damages the dielectric insulation performance, eventually triggering insulation breakdown accidents and directly threatening the safe and stable operation of capacitors [22-25]. Accordingly, investigating the insulation failure mechanism and PD characteristics of BOPP films is of great significance for identifying fault causes of filter bay capacitors and improving the overall operational reliability of UHV converter stations.

Extensive studies have been conducted by scholars worldwide [26-27]. Xi et al. investigated the partial discharge characteristics of biaxially oriented polypropylene (BOPP) films under pulsed electric fields [28]; Tong et al. studied the electro-thermal lifetime characteristics of metallized film capacitors under AC-DC superimposed conditions [12]. However, systematic research on the insulation failure mechanism and PD characteristics of BOPP films under power-frequency voltage superimposed with high-frequency harmonics remains insufficient.

To address this research gap, this study takes BOPP films as the research object, builds an electro-thermal combined-stress experimental platform, and systematically investigates the insulation failure mechanisms and partial discharge characteristics of BOPP films under combined characteristic- and high-frequency-harmonic stresses. The Methods section describes the experimental platform and test procedures, while the Results section examines the effects of harmonic frequency, harmonic proportion, and ambient temperature on breakdown and partial discharge behavior.

2 Methods

2.1 Experimental Platform

As illustrated in Figure 1, the electro-thermal composite stress experimental platform comprises a signal generator, power amplifier, current-limiting resistor, sphere-plane electrode, constant-temperature forced-air drying oven, high-frequency current probe, high-voltage probe, partial discharge (PD) detector, and digital oscilloscope. This setup supports the output of power-frequency voltage superimposed with high-frequency harmonics, precise ambient temperature control, and synchronous signal acquisition.

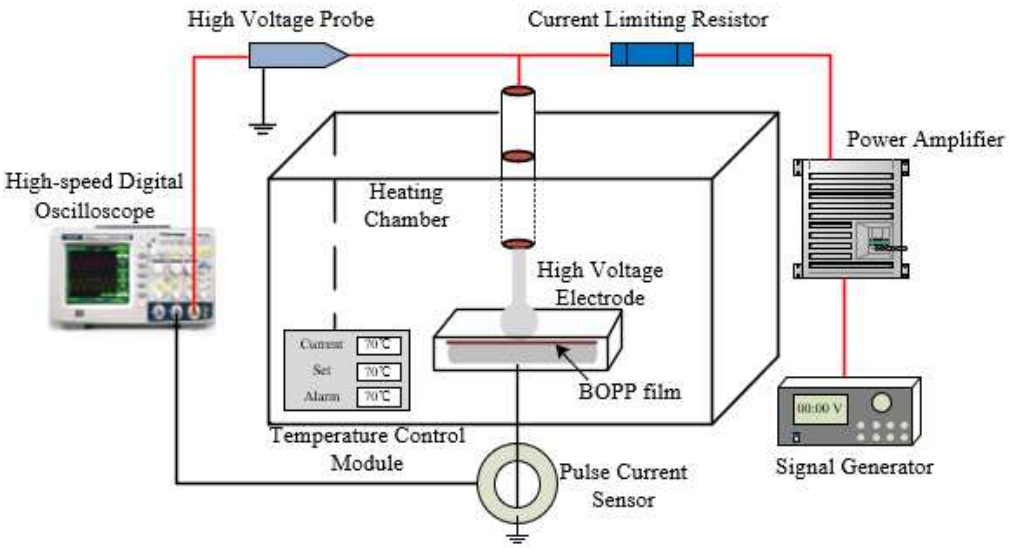


Figure 1. *Electro-thermal combined stress experimental platform.*

During the experiments, the BOPP film was first laid flat between the high-voltage electrode and ground electrode, and the entire electrode-specimen assembly was immersed in transformer oil to replicate the actual operating conditions of BOPP films. Prior to each test, the position of the high-voltage electrode was adjusted to ensure intimate contact with the BOPP film, thereby eliminating interfacial air gaps.

The BOPP film specimens used in this study were commercially produced dielectric films supplied by Wuxi Lianda Electric Co., Ltd., with a nominal thickness of 15 μm. Before testing, all specimens were uniformly cut into 100 mm×100 mm squares with smooth, burr-free edges, to avoid mechanical wrinkles and surface contamination on the specimens and rule out interference from pre-existing defects on the measurement results.

The ground electrode was an aluminum plate with a radius of 400 mm and a thickness of 10 mm. The entire electrode assembly was placed on a 10 mm-thick epoxy resin board, housed inside the constant-temperature forced-air drying oven, and connected to external circuits via lead wires.

Before voltage application, the specimens were preheated in the forced-air oven. After reaching the preset temperature, the thermal condition was maintained for at least 1 h to ensure a uniform and stable internal temperature throughout the specimens. Once the temperature stabilized, voltage was applied to the specimens via the signal generator. The high-voltage pulse power supply has an output voltage range of 0-50 kV, and both the voltage frequency and harmonic proportion are precisely regulated by the signal generator.

2.2 Experimental Methods

To systematically investigate the insulation failure mechanism and partial discharge characteristics of BOPP films under characteristic and high-frequency harmonics, this study took power-frequency voltage as the baseline condition and adopted the control variable method to examine the influences of harmonic frequency, harmonic proportion, and ambient temperature respectively.

The experimental parameters were determined in accordance with the actual operating characteristics of the filter bay in ultra-high voltage (UHV) converter stations. For harmonic parameters, 11th-order (550 Hz) and 13th-order (650 Hz) characteristic harmonics, as well as 10 kHz and 20 kHz high-frequency harmonics were selected, with three harmonic proportion levels (1%, 3%, and 5%) set for each frequency [29]. Considering the actual operating temperature of capacitors and the rated operating temperature as well as short-term maximum operating temperature of BOPP films, four temperature gradients were set in this study: 45 ℃, 55 ℃, 70 ℃, and 85 ℃ [30].

The breakdown characteristic tests of BOPP films were performed using the linear voltage ramp method. By adjusting the signal generator to output power-frequency voltage superimposed with high-frequency harmonics, the voltage was increased at a ramp rate of 500 V/s until specimen breakdown occurred, and the root-mean-square (RMS) value of the critical breakdown voltage was recorded synchronously. Ten test points were measured for each operating condition.

Partial discharge inception voltage (PDIV) tests were conducted using the stepwise voltage boosting method. The voltage was increased linearly at a rate of 500 V/s and held steady for 30 s at each voltage step. Partial discharge inception was confirmed when three or more consecutive valid discharge pulses with amplitudes above the background noise level were observed. The RMS value of the applied voltage at this point was recorded as the PDIV under the corresponding operating condition, along with relevant partial discharge data.

3 Results

3.1 Analysis of Breakdown Characteristics

3.1.1 Effect of Characteristic Harmonics

To investigate the influence of characteristic harmonics on the breakdown characteristics of BOPP films, experiments were performed at 45 ℃ to measure the characteristic

breakdown field strengths of BOPP films under power-frequency voltage superimposed with 11th-order and 13th-order characteristic harmonics at different harmonic proportions, and the results were compared with those obtained under pure power-frequency voltage.

Figure 2 shows the measured breakdown field strengths of BOPP films under power-frequency voltage superimposed with 11th-order characteristic harmonics of varying proportions.

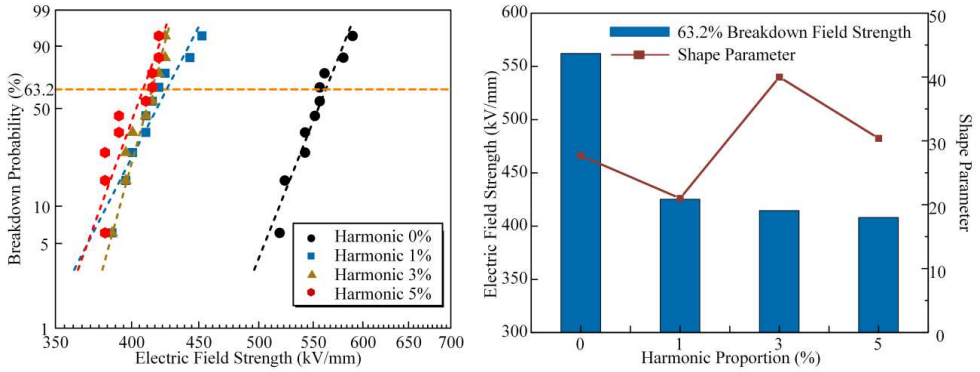


Figure 2. *Breakdown characteristics of different proportions of 11th characteristic harmonics.*

The breakdown voltage data were statistically processed using the Weibull distribution, yielding the characteristic breakdown field strength at a 63.2% breakdown probability and the corresponding shape parameter. By definition, the shape parameter characterizes the dispersion of breakdown data: a larger shape parameter indicates lower data scatter.

As shown in Figure 2, the breakdown field strength of BOPP films generally decreases with increasing superposition proportion of the 11th-order characteristic harmonic. Under power-frequency voltage, the characteristic breakdown field strength of BOPP films is approximately 562.2 kV/mm. At a 1% harmonic proportion, the value drops to 425.3 kV/mm. At a 3% harmonic proportion, the value drops to 414.6 kV/mm. The most significant reduction occurs at a 5% proportion, where the characteristic breakdown field strength reaches 408.2 kV/mm.

Meanwhile, the shape parameter exhibits a upward trend with rising characteristic harmonic proportion, indicating a notable reduction in the dispersion of the breakdown data.

Figure 3 presents the measured breakdown field strengths of BOPP films under power-frequency voltage superimposed with 13th-order characteristic harmonics at different proportions.

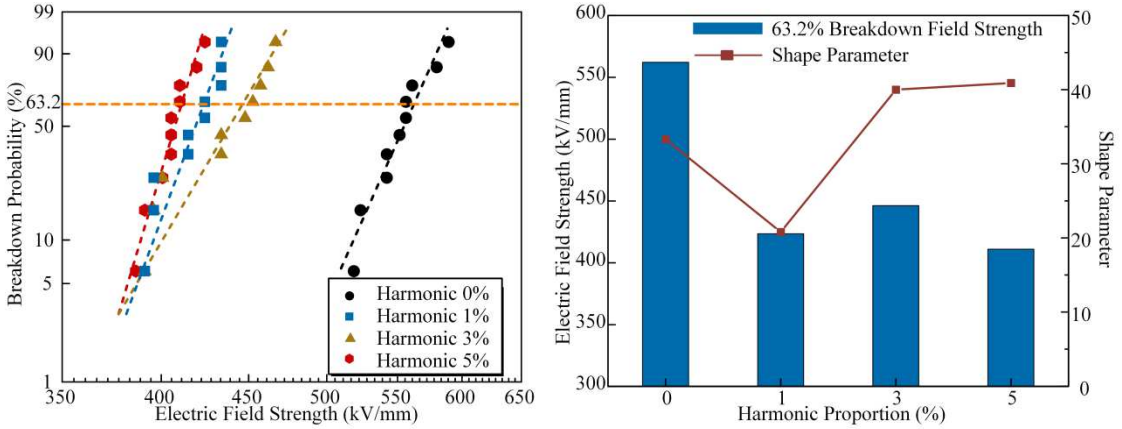


Figure 3. *Breakdown characteristics of different proportions of 13th characteristic harmonics.*

As shown in Figure 3, the characteristic breakdown field strength of BOPP films exhibits a trend of initial decrease followed by an increase with the rising proportion of the superimposed 13th-order characteristic harmonic. The minimum value of 411.1 kV/mm occurs at a harmonic proportion of 5%. At a 1% proportion, the characteristic breakdown field strength reaches 423.5 kV/mm, and the value further rises to 446.3 kV/mm when the proportion increases to 3%.

Meanwhile, the shape parameter presents a steady upward trend as the characteristic harmonic proportion grows, indicating a notable reduction in the dispersion of the breakdown data.

3.1.2 Effect of High-Frequency Harmonics

To investigate the influence of high-frequency harmonics on the breakdown characteristics of BOPP films, experiments were performed at 45 ℃ to measure the characteristic breakdown field strengths of BOPP films under power-frequency voltage superimposed with 10 kHz and 20 kHz harmonics at different harmonic proportions, and the results were compared with those obtained under power-frequency voltage.

Figure 4 shows the measured breakdown field strengths of BOPP films under power-frequency voltage superimposed with 10 kHz high-frequency harmonics of varying proportions.

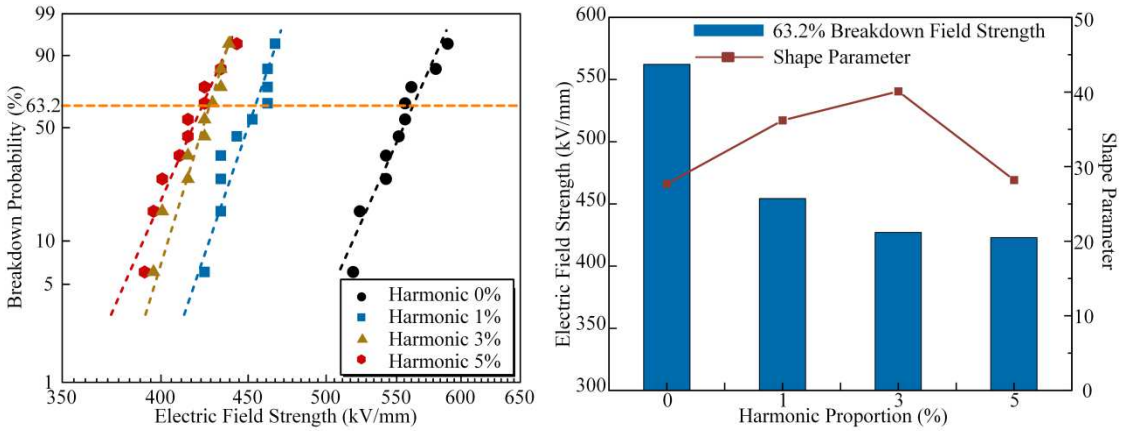


Figure 4. *Breakdown characteristics of 10 kHz high-frequency harmonics at different proportions.*

As shown in Figure 4, the characteristic breakdown field strength of BOPP films exhibits a decreasing trend with the rising proportion of the superimposed 10 kHz high-frequency harmonic. At a harmonic proportion of 1%, the characteristic breakdown field strength of BOPP films is 454.3 kV/mm; at a 3% proportion, the value drops to 427.1 kV/mm; the most significant reduction occurs at a 5% proportion, where the characteristic breakdown field strength drops to 422.9 kV/mm.

Meanwhile, the shape parameter presents a trend of initial increase followed by a decrease as the high-frequency harmonic proportion grows, indicating that the dispersion of breakdown data first decreases and then increases, with the lowest data scatter observed at a 3% harmonic proportion.

Figure 5 presents the measured breakdown field strengths of BOPP films under power-frequency voltage superimposed with 20 kHz high-frequency harmonics at different proportions.

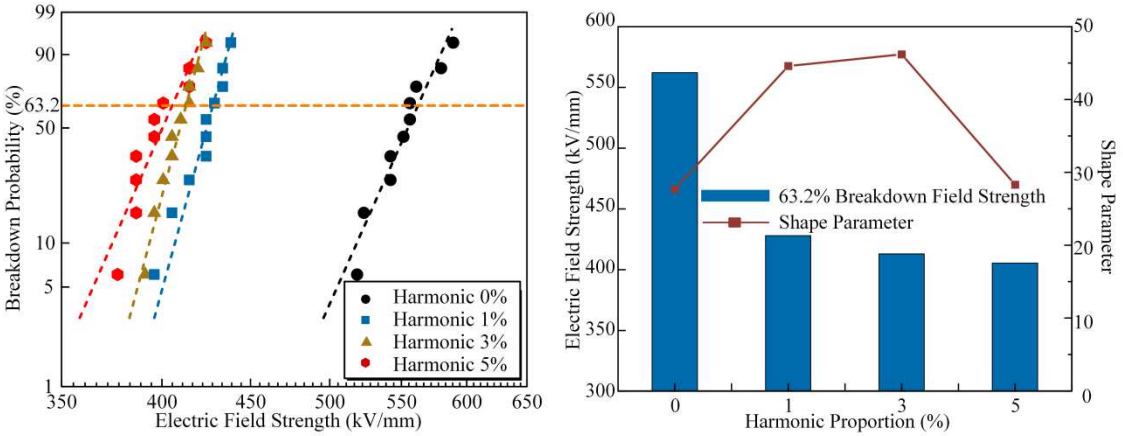


Figure 5. *Breakdown characteristics of 20 kHz high-frequency harmonics at different proportions.*

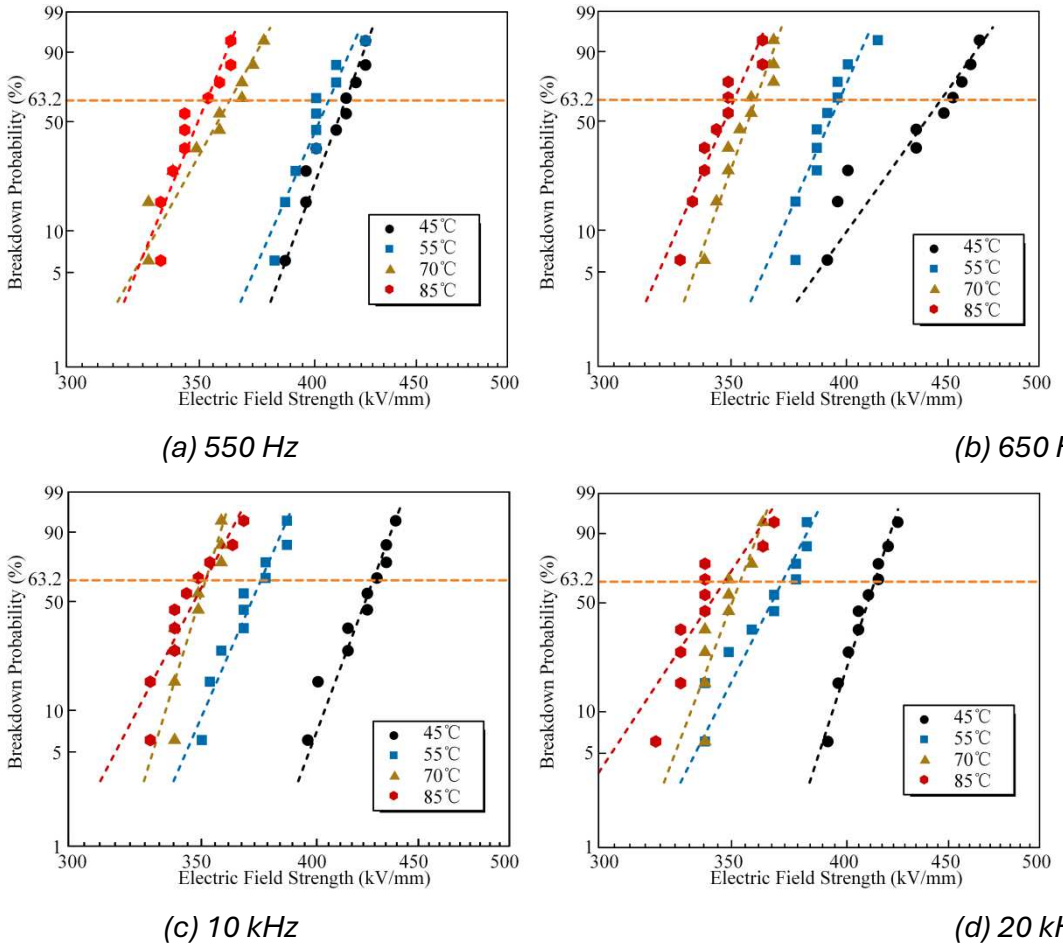
As shown in Figure 5, the characteristic breakdown field strength of BOPP films shows a downward trend with the increasing proportion of the superimposed high-frequency harmonic. At a harmonic proportion of 1%, the characteristic breakdown field strength of BOPP films is 428 kV/mm; at a 3% proportion, the value drops to 413 kV/mm; the minimum characteristic breakdown field strength of 405.5 kV/mm is reached at a 5% proportion.

For the shape parameter, it first increases and then decreases with the rising proportion of the 20 kHz high-frequency harmonic, with the lowest breakdown data scatter achieved at a 3% harmonic proportion.

Overall, under the same temperature and harmonic proportion conditions, a higher harmonic frequency corresponds to a lower breakdown field strength of BOPP films and more severe insulation degradation. This phenomenon may be attributed to the fact that high-frequency harmonics significantly increase the dielectric loss of BOPP films, while rising frequency intensifies the hysteresis effect of the dielectric polarization process. The heat generated by dielectric loss further accelerates the combined electro-thermal degradation of BOPP films.

3.1.3 Effect of Ambient Temperature

To further investigate the influence of ambient temperature on the breakdown characteristics of BOPP films, the control variable method was adopted with a fixed harmonic proportion of 3%. Breakdown characteristic tests were conducted under three voltage conditions: pure power-frequency voltage, power-frequency voltage superimposed with characteristic harmonics, and power-frequency voltage superimposed with high-frequency harmonics, across four temperature gradients of 45 ℃, 55 ℃, 70 ℃, and 85 ℃. The results are shown in Figure 6.



(a) 550 Hz *(b) 650 Hz*

(c) 10 kHz *(d) 20 kHz*

Figure 6. *Breakdown characteristics at different temperatures.*

As shown in Figure 6, under all test conditions, the characteristic breakdown field strength of BOPP films consistently exhibits a downward trend with rising ambient temperature. When the temperature increases from 45 ℃ to 85 ℃, under the 11th-order characteristic harmonic condition, the characteristic breakdown field strength drops from 414.6 kV/mm to 252.9 kV/mm; under the 13th-order characteristic harmonic condition, the value decreases from 446.3 kV/mm to 351.2 kV/mm; under the 10 kHz high-frequency harmonic condition, the value reduces from 427.1 kV/mm to 351.6 kV/mm; under the 20 kHz high-frequency harmonic condition, the value falls from 413 kV/mm to 347.1 kV/mm. It can be observed that ambient temperature exerts the most significant influence on the breakdown field strength under the 11th-order characteristic harmonic condition.

3.2 Analysis of Partial Discharge Inception Field Strength

3.2.1 Effect of Characteristic Harmonics

To further investigate the influence of characteristic harmonics on the partial discharge characteristics of BOPP films, experiments were conducted at 45 ℃ to measure the characteristic partial discharge inception field strengths of BOPP films under power-

frequency voltage superimposed with 11th-order and 13th-order characteristic harmonics, and the results were compared with those obtained under pure power-frequency voltage. Figure 7 presents the measured partial discharge inception field strengths of BOPP films under power-frequency voltage superimposed with 550 Hz (11th-order) harmonics at different proportions.

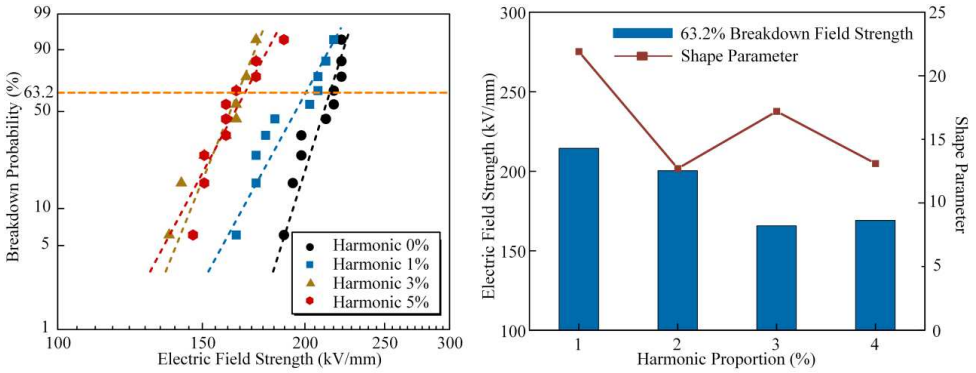


Figure 7. *Partial discharge characteristics of different proportions of 11th characteristic harmonics.*

The partial discharge (PD) inception field strength data were statistically processed using the Weibull distribution, yielding the characteristic PD inception field strength at a 63.2% inception probability and the corresponding shape parameter. By definition, the shape parameter characterizes the dispersion of PD inception data: a larger shape parameter indicates lower data scatter.

As shown in Figure 7, the PD inception field strength of BOPP films exhibits a trend of initial decrease followed by an increase with the rising proportion of the superimposed 11th-order characteristic harmonic. Under power-frequency voltage, the characteristic PD inception field strength is 214.4 kV/mm. At a 1% proportion, the PD inception field strength reaches 200.4 kV/mm, the minimum value of approximately 165.7 kV/mm occurs at a harmonic proportion of 3%, and the value further rises to 169.1 kV/mm when the proportion increases to 5%. Meanwhile, the shape parameter exhibits a marked upward trend with rising characteristic harmonic proportion, indicating a notable reduction in the dispersion of the PD inception data.

Figure 8 presents the experimental results of the partial discharge inception field strength of BOPP films under power-frequency voltage superimposed with 13th-order characteristic harmonics at different proportions.

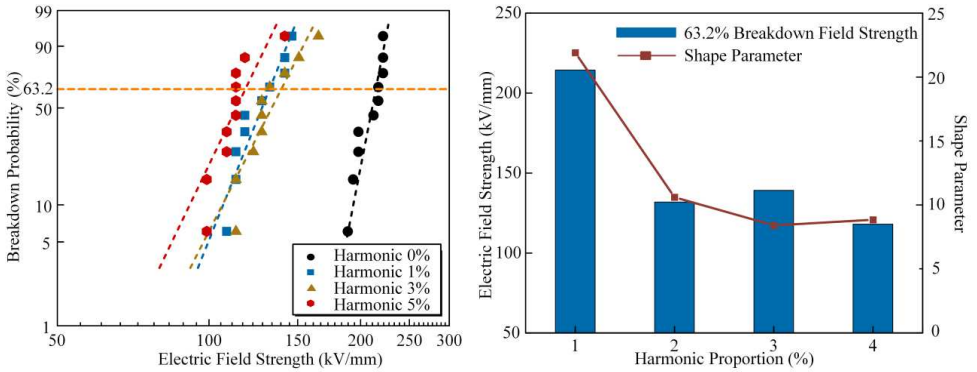


Figure 8. *Partial discharge characteristics of different proportions of 13th characteristic harmonics.*

As shown in Figure 8, the characteristic PD inception field strength of BOPP films exhibits a trend of initial decrease followed by an increase with the rising proportion of the superimposed 13th-order characteristic harmonic. The minimum value of 131.9 kV/mm occurs at a harmonic proportion of 1%. At a 3% proportion, the characteristic PD inception field strength rises to 139.2 kV/mm, while the value drops to 118.1 kV/mm at a 5% proportion.

Meanwhile, the shape parameter presents a marked downward trend as the characteristic harmonic proportion increases, indicating a significant increase in the dispersion of PD inception data. Compared with the 11th-order characteristic harmonic, the 13th-order characteristic harmonic exerts a more significant influence on the characteristic PD inception field strength of BOPP films, and may induce more severe insulation degradation.

3.2.2 Effect of High-Frequency Harmonics

To further investigate the influence of high-frequency harmonics on the PD characteristics of BOPP films, experiments were conducted at 45 ℃ to measure the characteristic PD inception field strengths of BOPP films under power-frequency voltage superimposed with 10 kHz and 20 kHz harmonics at different harmonic proportions, and the results were compared with those obtained under power-frequency voltage.

Figure 9 presents the measured PD inception field strengths of BOPP films under power-frequency voltage superimposed with 10 kHz high-frequency harmonics at varying proportions.

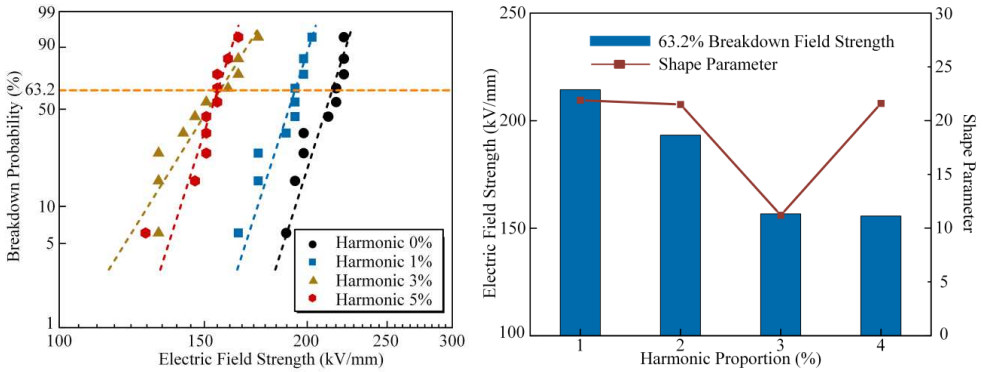


Figure 9. *PD characteristics of 10 kHz high-frequency harmonics at different proportions.*

As shown in Figure 9, the characteristic PD inception field strength of BOPP films exhibits a downward trend with the rising proportion of the superimposed 10 kHz high-frequency harmonic. The value of 193.3 kV/mm occurs at a harmonic proportion of 1%. At a 3% proportion, the characteristic PD inception field strength drops to 156.7 kV/mm, and the minimum value of 155.7 kV/mm is reached at a 5% proportion.

It can be concluded that the proportion of the 10 kHz high-frequency harmonic has a significant influence on the PD inception field strength of BOPP films, and the influence becomes more pronounced with increasing harmonic proportion.

Meanwhile, the shape parameter exhibits a shows a trend of decreasing and then increasing as the proportion of high-frequency harmonics rises, which indicates that the dispersion of PD inception test data first increases and then decreases.

Figure 10 presents the measured PD inception field strengths of BOPP films under power-frequency voltage superimposed with 20 kHz high-frequency harmonics at different proportions

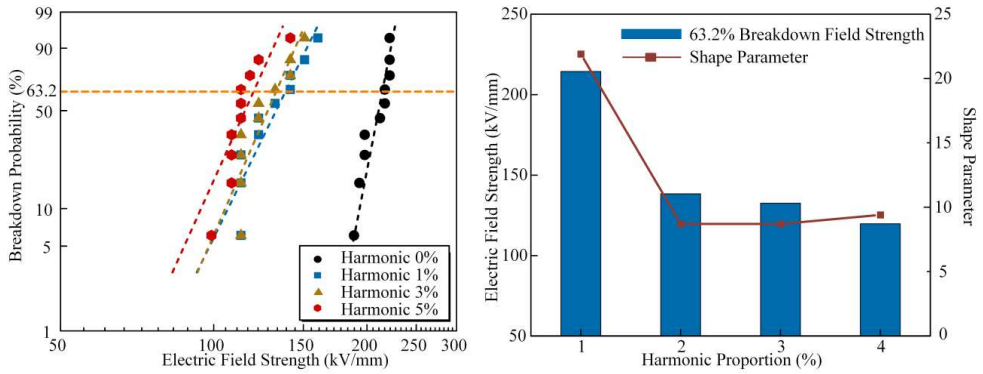


Figure 10. *PD characteristics of 20 kHz high-frequency harmonics at different proportions.*

As shown in Figure 10, the characteristic PD inception field strength of BOPP films shows a gradual downward trend with the increasing proportion of the superimposed 20 kHz high-frequency harmonic. At a harmonic proportion of 1%, the characteristic PD inception field strength of BOPP films is 138.4 kV/mm. The most significant reduction occurs at a 3%

proportion, where the value drops to 132.6 kV/mm, and the minimum characteristic PD inception field strength of 119.8 kV/mm is reached at a 5% proportion.

Meanwhile, the shape parameter exhibits a downward trend with rising harmonic proportion, indicating a significant increase in the dispersion of PD inception data.

3.2.3 Effect of Ambient Temperature

To investigate the influence of ambient temperature on the PD inception field strength of BOPP films, the control variable method was adopted with a fixed harmonic proportion of 3%. PD inception field strength tests were conducted under two voltage conditions: power-frequency voltage superimposed with characteristic harmonics and power-frequency voltage superimposed with high-frequency harmonics, across three temperature gradients of 55 ℃, 70 ℃, and 85 ℃.

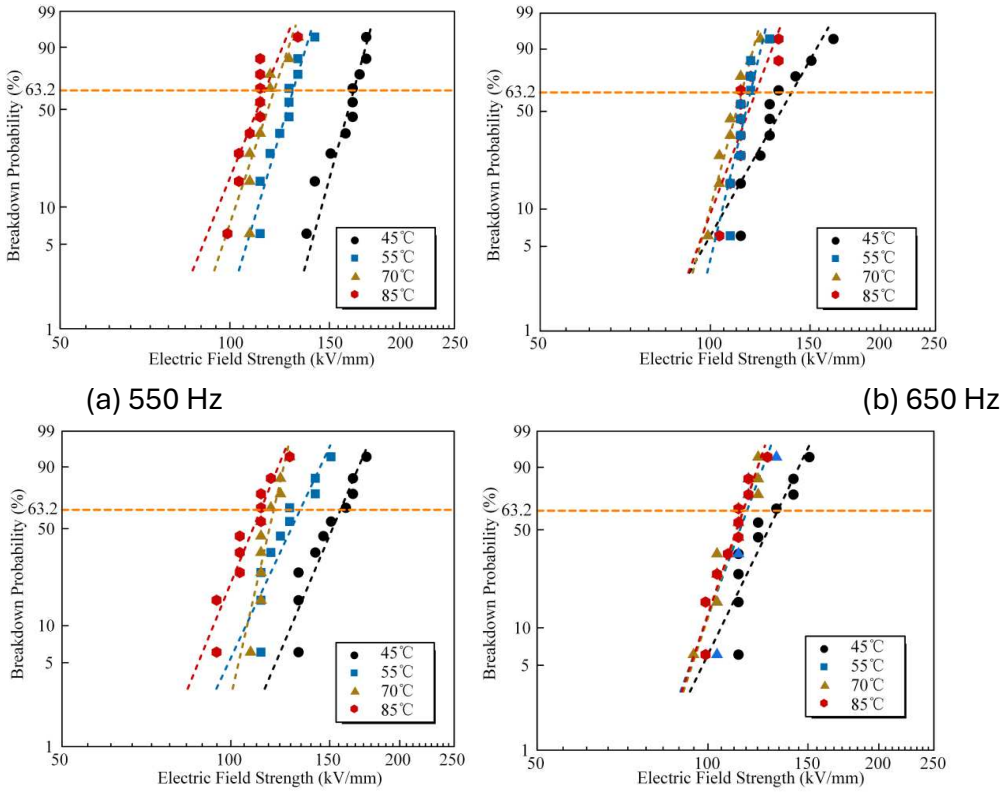


Figure 11. *PD characteristics at different temperatures.*

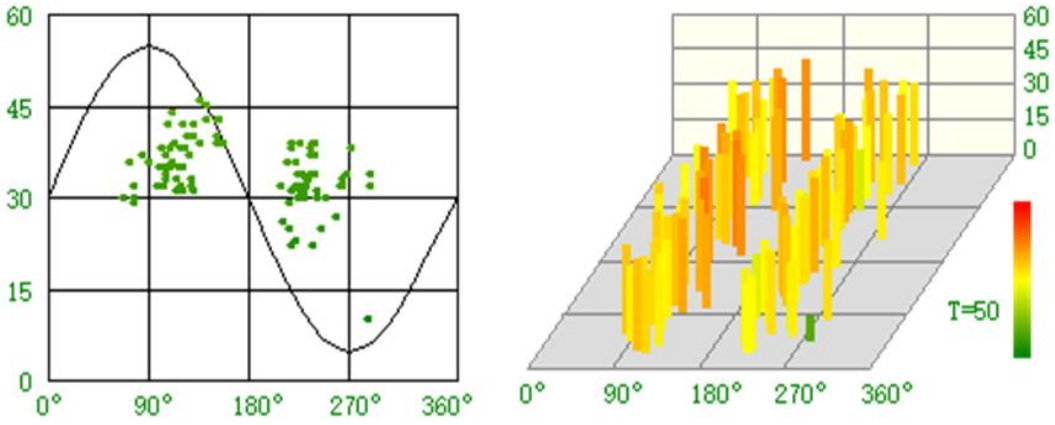
3.3 Analysis of Partial Discharge Characteristics

To further investigate the influence pattern of voltage waveform distortion on the partial discharge characteristics of BOPP films, experiments were conducted under the test conditions of 70 ℃ and a fixed 3% harmonic proportion. Partial discharge signals were acquired under three voltage conditions: pure power-frequency voltage, power-frequency voltage superimposed with characteristic harmonics, and power-frequency voltage

superimposed with high-frequency harmonics. A comparative analysis of the measured data was performed using the phase-resolved partial discharge (PRPD) pattern and the phase-resolved pulse sequence (PRPS) pattern.

3.3.1 Partial Discharge under Power-Frequency Voltage

The PRPD pattern and PRPS pattern of BOPP films under power-frequency voltage are presented in Figure 12.



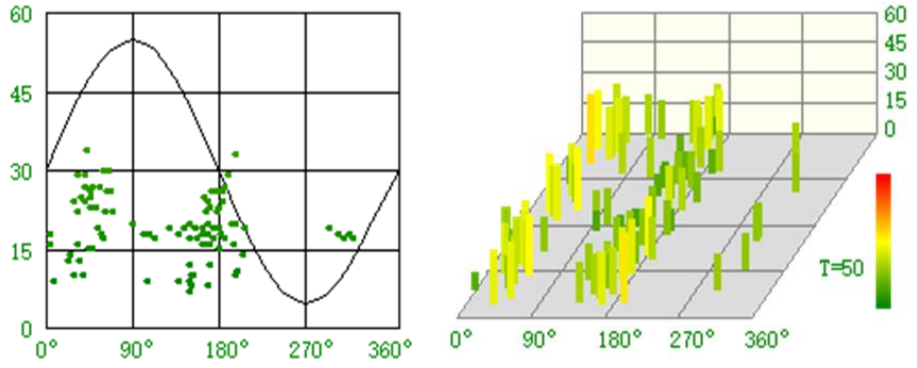
(a) PRPD *(b) PRPS*

Figure 12. *PD characteristics under power-frequency voltage.*

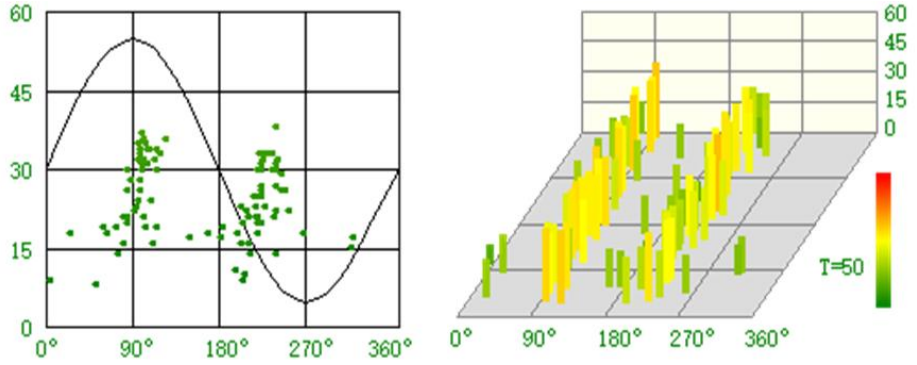
As illustrated in Figure 12, under power-frequency voltage, partial discharges of the BOPP film are concentrated within the phase range of 70°–150° during the positive half-cycle, featuring dense scatter points and generally high discharge amplitudes with obvious power-frequency periodicity. In the negative half-cycle, PD activities mainly occur from 210° to 300°, and the overall discharge amplitude is slightly lower than that in the positive half-cycle.

3.3.2 Partial Discharge under Characteristic Harmonics

The PRPD and PRPS patterns of BOPP films under power-frequency voltage superimposed with characteristic harmonics are shown in Figure 13.



550 Hz



650 Hz

Figure 13. *Partial discharge characteristics under power-frequency voltage superimposed with characteristic harmonics.*

As shown in Figure 13(a), when power-frequency voltage is superimposed with 550 Hz harmonics, the partial discharge (PD) of BOPP films distributes across the entire positive half-cycle from 0° to 180°, with two dense discharge clusters emerging in the ranges of 0°–60° and 80°–180°. Only a small number of low-amplitude discharges occur in the negative half-cycle within 270°–360°, and the overall PD activities are dominated by the positive half-cycle. Compared with the condition of pure power-frequency voltage, the overall discharge amplitude decreases, and the proportion of low-amplitude pulses increases remarkably.

As shown in Figure 13(b), under power-frequency voltage superimposed with 650 Hz harmonics, obvious discharge clusters are formed in both the positive and negative half-cycles. PD signals are concentrated in the positive half-cycle from 60° to 140°, while discharges in the negative half-cycle mainly fall within 200°–280°. A small number of leading pulses can be observed, and discharges still predominantly take place near the voltage peak. Although the PD activities exhibit a certain degree of symmetry between the two half-cycles, the symmetry is weaker than that under pure power-frequency voltage.

3.3.3 Partial Discharge under High-Frequency Harmonics

The PRPD and PRPS patterns of BOPP films under power-frequency voltage superimposed with high-frequency harmonics are shown in Figure 14.

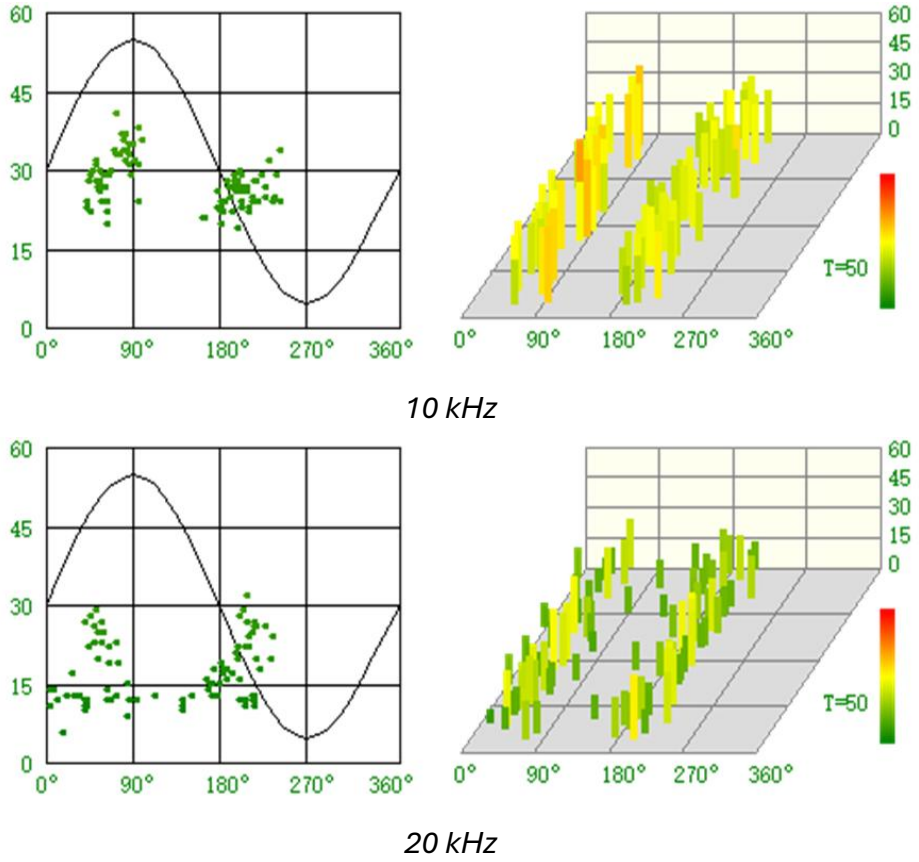


Figure 14. *PD characteristics under power-frequency voltage superimposed with high-frequency harmonics*.

As shown in Figure 14(a), under power-frequency voltage superimposed with 10 kHz harmonics, one concentrated discharge cluster is formed respectively in the positive and negative half-cycles. Discharges in the positive half-cycle are distributed from 30° to 110°, while those in the negative half-cycle are concentrated within 180°–250°. Compared with power-frequency voltage, the inception phase of partial discharges shifts forward. The discharge distribution shows an overall symmetric structure between the two half-cycles, yet the symmetry is inferior to that under power-frequency voltage. Partial discharge pulses are highly concentrated, and the overall discharge amplitude is slightly lower.

As shown in Figure 14(b), obvious discharge clusters can be observed in both half-cycles when 20 kHz harmonics are superimposed on the power-frequency voltage. Positive-half-cycle discharges are located in the range of 0°–100° with a remarkably advanced inception phase, and negative-half-cycle discharges mainly fall within 170°–240°. The overall discharge amplitude is lower than that under power-frequency voltage, with a large proportion of low-amplitude pulses.

4 Conclusion

This study focuses on biaxially oriented polypropylene (BOPP) films used in parallel capacitors of circuit breakers in ultra-high-voltage (UHV) converter stations. A series of breakdown and partial discharge (PD) tests are systematically carried out by establishing an electro-thermal experimental platform, covering pure power-frequency voltage, power-frequency voltage superimposed with typical characteristic harmonics (550 Hz and 650 Hz) and high-frequency harmonics (10 kHz and 20 kHz), harmonic proportions ranging from 1% to 5%, and operating temperatures varying from 45 ℃ to 85 ℃. The coupling influences of harmonic frequency, harmonic proportion and temperature on the insulation failure characteristics of BOPP films are comprehensively investigated.

The experimental results indicate that superimposed harmonics significantly degrade the insulation performance of BOPP films. Within the tested conditions, both the characteristic breakdown field strength and PD inception field strength under harmonic superimposed voltages are generally lower than those under pure power-frequency voltage. Under characteristic harmonic excitation, the insulation parameters exhibit non-monotonic variation with the increase of harmonic proportion. For high-frequency harmonic conditions, the insulation deterioration is more severe, and the field strengths obtained at 20 kHz are consistently lower than those at 10 kHz under the same harmonic proportion.

Elevated temperature further exacerbates the insulation degradation under electro-thermal coupled stress. The characteristic breakdown field strength decreases monotonically with rising temperature under all harmonic conditions, while the PD inception field strength generally declines with increasing temperature but presents partial overlapping and non-monotonic variation in certain temperature intervals. In addition, harmonic fields significantly reduce the PD inception field strength, which decreases continuously with the growth of harmonic proportion under high-frequency harmonics.

The phase-resolved partial discharge (PRPD) and phase-resolved pulse sequence (PRPS) patterns vary obviously with voltage waveforms. Pure power-frequency voltage yields symmetric and highly periodic PD distributions. The superposition of characteristic harmonics broadens the PD phase range, weakens phase symmetry, and increases the quantity of low-amplitude discharge pulses. When high-frequency harmonics are introduced, the PD inception phase shifts forward remarkably, and the dispersion of discharge pulses increases significantly. This study provides a reliable theoretical basis for insulation condition evaluation and fault prevention of parallel capacitors in UHV converter stations.

Acknowledgements

This research was funded by State Grid Shandong Electric Power Company, grant number 2025A-078, project title: Research on Insulation Failure Mechanism and Condition

Assessment Technology of Shunt Capacitors for Circuit Breakers in Converter Station Filter Yard under Complex Operating Conditions.

Author contributions statement

Conceptualization and original draft preparation, X. W.; methodology, formal analysis and review editing, M. Z.; resources, supervision, project administration and funding acquisition, Q. Z.; investigation, data curation and visualization, L. L. All authors have read and agreed to the published version of the manuscript.

Data availability

All data supporting the findings of this study are available within the paper. All original experimental data, characteristic parameter analysis data, partial discharge test results and insulation failure characterization data involved in this study have been fully presented in the manuscript text, figures, and tables. No undisclosed core data related to the research conclusions exists.

Additional information

Competing interests

The authors declare no competing interests.

References

1. Heidary, A.; Radmanesh, H.; Bakhshi, A.; Rouzbehi, K.; Pouresmaeil, E. A Compound Current Limiter and Circuit Breaker. Electronics. 2019, 8, 551.
2. Zhong, L.; Liu, K. Visual Classification and Detection of Power Inspection Images Based on Federated Learning. IEEE Trans. Ind. Appl. 2024, 60, 4, 5460–5469.
3. Cai, H.; Zhang, J.; Yu, J.; Zhang, Z. Fault Current and Voltage Estimation for Pole-to-Pole Faults in Modular Multilevel Converter Based DC Grids Considering AC Active Power. Appl. Sci. 2021, 11, 2882.
4. Du, G.; Zhang, J. Capacitance Evaluation of Metallized Polypropylene Film Capacitors Considering Cumulative Self-Healing Damage. Electronics. 2024, 13, 2886.
5. Guo, Y.; Yuan, B.; Zhou, B.; Li, T. Generation Mechanism and Suppression Measures of Flexible DC Converter Ultra-High Frequency Harmonic. In Proceedings of the 2026 IEEE 9th International Electrical and Energy Conference (CIEEC), Tianjin, China, 2026.
6. Căiman, D.-V.; Bărbulescu, C.; Nanu, S.; Dragomir, T.-L. DC-DC Buck Converters with Quasi-Online Estimation of Filter Capacitor Equivalent Parameters. Appl. Sci. 2024, 14, 10756.

7. Shaw, D.G.; Cichanowski, S.W.; Newcomb, G.R.; Yializis, A. Electrical Properties and Aging Mechanisms in Metallized Polypropylene Film Capacitors. In Proceedings of the 1982 IEEE International Conference on Electrical Insulation, Philadelphia, PA, USA, 1982.

8. Zuo, Q.; Zhao, Y.; Han, X. Research on Application of Self-Healing Metallized Film Capacitors of DC Filter for HVDC System. In Proceedings of the 2024 International Conference on HVDC (HVDC), Urumqi, China, 2024; pp. 347–354.

9. Song, J.; et al. Influence of Multi-Physical Fields Aging on the Insulation Properties of BOPP Films for Dry DC Capacitors. In Proceedings of the 2025 IEEE Conference on Electrical Insulation and Dielectric Phenomena (CEIDP), Manchester, United Kingdom, 2025; pp. 68–71.

10. Liang, C.; et al. A Multicell SCC Capacitive Coupler With Strong Lateral, Longitudinal, and Rotational Antioffset Performance. IEEE Trans. Power Electron. 2025, 40, 4, 6230–6247.

11. Chen, F.; et al. In-situ Measurement and Characterization of Self-Healing Processes in Biaxially Oriented Polypropylene (BOPP) Metallized Film Capacitors. In Proceedings of the 2025 26th International Conference on Electronic Packaging Technology (ICEPT), Shanghai, China, 2025; pp. 1–5.

12. Tong, Y.; Chen, G.; Liu, X.; Wang, C.; Tu, Y. AC-DC Superimposed Breakdown Characteristics and Evaluation Methodology for Converter Valve Capacitor Films. IEEE Trans. Dielectr. Electr. Insul. 2026, in press.

13. Chen, K.; Du, B.X.; Liu, H.; Xiao, M. Improved Dielectric and Energy Storage Performance of BOPP Film by Decreasing Ambient Temperature. IEEE Trans. Dielectr. Electr. Insul. 2025, 32, 1056–1063.

14. Chen, Y.; Mi, Y.; Liu, C.; Liu, W.; Peng, Y.; Liao, R. Effect of Temperature on Partial Discharge Characteristics of BOPP Film Under Nanosecond Pulse Voltage. IEEE Trans. Dielectr. Electr. Insul. 2024, 31, 3031–3039.

15. Lu, J.; Zhu, B.; Zhang, X.; Wang, X. Dielectric Strength Structure-Activity Relationship of BOPP Film for High Energy Density Pulse Capacitor. IEEE Trans. Plasma Sci. 2019, 47, 4342–4349.

16. Mi, Y.; Chen, Y.; Liu, C.; Zhu, Y.; Liao, R. Partial Discharge Characteristics of Biaxially Oriented Polypropylene Film Under Nanosecond Pulse Voltage With High Rise Rate. IEEE Trans. Plasma Sci. 2023, 51, 498–506.

17. Wang, X.; Huang, L.; Song, Y.; et al. Microstructure Evolution of Uniaxially Stretched Polypropylene Film and Its Influence on Electrical Properties. High Volt. Eng. 2025, 51, 2260–2267.(in Chinese).

18. Zhang, C.S.; Zhang, C.; Ren, C.Y.; et al. Research Progress on Influence Mechanisms and Optimization Strategies for Energy Storage in Polypropylene-Based Films. Trans. China Electrotech. Soc. 2024, 39, 2193–2213.(in Chinese).

19. Ritamäki, M.; Rytöluoto, I.; Lahti, K.; et al. Large-Area Approach to Evaluate DC Electro-Thermal Ageing Behavior of BOPP Thin Films for Capacitor Insulation Systems. IEEE Trans. Dielectr. Electr. Insul. 2017, 24, 826–836.

20. Zheng, J.; Huang, B.; Chen, G.; Zhang, C.; Zhao, Z.; Zhong, S.; Shao, T.; Tu, Y. High-resolution space charge distribution in micro-scale dielectric films. Communications Materials. 2025, 6, 1, 156.

21. Yang, M.; Wan, C.; Zhou, L.; Li, X.; Pan, J.; Li, H.; Wang, J.; Ren, W.; Sun, B.; Xu, E.; Xiao, Y.; Guo, M.; Zhang, M.; Li, X.; Jiang, J.; Hu, P.; Duan, L.; Nan, C.-W.; Shen, Z.; Wang, X.; Shen, Y. High-temperature polymer composite capacitors with high energy density designed via machine learning. Nature Energy. 2025, 10, 11, 1323–1333.

22. Zhang, S.T.; Tian, F.Q.; Cao, J.M.; et al. Thermal Aging Life Model of Biaxially Oriented Polypropylene Films for Capacitors Based on Cumulative Power Energy Absorption. Polymer 2024, 313, 127722.

23. Zhang, C.S.; Feng, Y.; Kong, F.; et al. Accelerated Damage in Metallized Film Capacitors Under Pulse Surge Combined With Rated DC Voltage. IEEE Trans. Plasma Sci. 2023, 51, 1494–1501.

24. He, Y.S.; Wang, F.P.; Du, G.Q.; et al. Revisiting the Thermal Ageing on the Metallised Polypropylene Film Capacitor: From Device to Dielectric Film. High Volt. 2023, 8, 305–314.

25. Feng, M.; Jia, Z.; Liu, Y.; Liu, Y.; Shi, J.; Zhao, C.; Sun, T.; Liu, H.; Xing, Y. Study on the Effect of Temperature on the Self-Healing Behavior of Film Capacitor Dielectrics. Materials 2025, 18, 4033.

26. Li, W.; Wang, Q.; Zhang, G.; He, Y.; Qin, B.; Zhang, X.; Liu, Z.; Gong, H.; Zhang, Z. Ultrahigh Energy Density Achieved at High Efficiency in Dielectric Capacitors by Regulating α-Phase Crystallization in Polypropylene Films with Fluorinated Groups. Adv. Funct. Mater. 2024, 34, 2410959.

27. Zhu, J.; Tong, H.; Cao, S.; Luo, J.; Liu, X.; Xu, J.; Oleksandr, M.; Peng, W. Self-healing behaviors of metallized high-temperature dielectric films for capacitor applications. Microelectron. Reliab. 2023, 144, 114972.

28. Mi, Y.; Chen, Y.; Liu, C.; Zhu, Y.; Liao, R. Partial Discharge Characteristics of Biaxially Oriented Polypropylene Film Under Nanosecond Pulse Voltage With High Rise Rate. IEEE Trans. Plasma Sci. 2023, 51, 498–506.

29. Gu, Z.; et al. Research on Harmonic Characteristics of Transformer Operation Under Frequent Switching of High-Proportion New Energy Access Trend. In Proceedings of the 2024 4th International Conference on Electrical Engineering and Control Science (IC2ECS), Nanjing, China, 2024; pp. 576–580.

30. Feng, M.; Jia, Z.; Liu, Y.; Liu, Y.; Shi, J.; Zhao, C.; Sun, T.; Liu, H.; Xing, Y. Study on the Effect of Temperature on the Self-Healing Behavior of Film Capacitor Dielectrics. Materials. 2025, 18, 4033.